Optimum process parameters for increasing the drawability of square cup though conical die

**Majdy Mostafa M. Abdelbarr[a], Ibrahim M. Hassab-Allah[b] , Ahmed Bayummi[a] ,
W.M. Shewakh[a,c*]**

[a] Industrial Engineering Department, Faculty of Engineering, Jazan University, KSA
[b] Department of Mechanical Engineering, Faculty of Engineering, Assiut University, Egypt
[c] Mechanical Production Department, Faculty of technology and Education, Beni-Suef University,
Beni-Suef, Egypt.
*Corresponding author E-mail: waleedshewakh@hotmail.com

ABSTRACT

The study introduces finite element simulation (FES) together with their corresponding experimental results for the square-cup deep drawing with simultaneous corrective ironing through conical die with no use of blank holder. The FES model has been used to investigate the optimum tool dimensions and process parameters. The independent variables of the investigation are the relative die clearances, material properties, sheet thickness, and punch surface roughness conditions. Relative die clearances of 1.5, 1.0, 0.9, 0.8 and 0.7 from the initial sheet thickness were used. The last four values (1.0, 0.9, 0.8 and 0.7) give simultaneous corrective ironing ratios 0, 10, 20, and 30% respectively. Three kinds of sheet metals; including half hard aluminum (Al99.5w), annealed aluminum and brass (67/33 Cu-Zn) with nominal sheet thickness of 1, 1.5, 2, 2.5 and 3 mm in each metal were used. In order to study the square cup deep drawing with a high coefficient of friction at the punch-blank interface, three punches were manufactured and knurled allover to give a rough surfaces finish. Grease as a lubricant was used in the die-blank interface only. The graphs of the results of the real experiments and FE simulation regarding the drawing loads, modes of failures, and LDR's indicate very good agreement between the two ways of analysis.

Keywords: Deep drawing of square cup, Conical die, Simultaneous corrective ironing, Optimum parameters, FE simulation, Limiting deep drawing ratios LDR's.

1.   INTRODUCTION

Square-cup deep drawing is a technology that is used in a wide range of production processes. Square cup deformation depends on the properties of the deformed metal and conditions of the interface between the tool and sheet. Used equipment, pattern of the metal flow, and plastic-deformation mechanics are also considerable factors [1]. Equipment and tooling parameters, upon which the success of square-cup deep drawing depends, include the drawing speed; lubrication conditions, method and force restraining the flow of blank metal (such as blank holding force or draw beads), radii of punch/die corners and edges, and punch/die clearance.

Two ways can be employed in order to increase the limiting drawing ratio, LDR, of the square-cup deep drawing. First way is to introduce improvements to the process parameters including the tool geometry and temperature, conditions of friction and lubrication, and blank shape [2-10]. On this first way, many researches investigating the effect of the tool shape and the lubrication conditions on the forming limit have been done [11-15].

The other way for increasing the LDR is to develop a new pattern of the metal flow of the blank [11]. On this second way, come many proposed methods targeting the enhancement of the formability of the square-cup deep drawing [5], [11,12]. One of these new methods is that has been proposed [17-21]. In that method a conical die ending

with a square aperture was used with the purpose of enabling the metal to flow easily from the cone circular sections to the square section of the ending aperture. As a result, there would be no need for draw beads and blank holding load. The load required for deformation has also been reduced and could be provided by a single-acting press.

The main objective of the present work is to study the influence of the main process parameters on the drawability of square cup as a means to determine their optimum values. These parameters are die dimensions, punch dimensions, die relative clearance, blank thickness, and friction conditions. Comparisons between FE simulation and experimental results are also conducted regarding the drawing loads, LDR's, modes of failure, distribution of cup thickness and distribution of cup height.

2. Experimental procedures and materials

2.1. Deep drawing apparatus

Figure 1 shows a photograph for the developed deep drawing apparatus. It is composed of three sets: upper, middle, and bottom. Upper set is a punch set, which is an assembly of a shaft, punch, and centering bolt. This set is mounted to the upper platen of a computerized hydraulic press. Concentricity of the to-be-positioned circular blank and the punch is achieved by the centering bolt. The middle is the die set. The main component of this set is the die, which is conical with 18° half cone-

angle. Rotation of the die is prevented by a die stock. The die set is assembled with the bottom set and the assembly is mounted to the bottom platen of the hydraulic press. The drawn cups are taken out through an orifice in the bottom set.

The test machine that has been used in the experiments is a computerized one with a data acquisition system, through which the load displacement is automatically stored, displayed, and printed. The machine is of maximum capacity 1000 kN with working piston stroke 225 mm. Experiments have been conducted at a rate of strain 8.33×10^{-5}/s. This rate guarantees a quasi-static deformation state and negligible strain-rate effect.

Figure1: Developed deep drawing apparatus.

2.2. Punches and die

A total of fifteen punches were used in the experimental work. Punches are made of special tool steel (210CrW12: 2%C and 12%Cr with Tungsten and Vanadium addition to improve wear resistance). The punches are of 230 mm length with flat heads, of which the profile and corner radii are 4 mm and 8 mm, respectively. Sides of the punch stems are tapped with 0.15^{o} taper angle that enables the drawn pieces remove out easily. The punches are

of 60-62 Rockwell-C hardness. Hardening has done by heating the punches to 980°C under vacuum then quenching in oil [22]. Grinding and polishing brought twelve of the punch stems to be with nominal square side lengths 35.0, 36.5, 38.0, 38.6, 39.0, 39.5, 39.8, 40.0, 40.4, 40.8, 41.2, and 42.0 mm. After grinding and polishing, the surface roughness of punches have attained a value of $R_a = 7.5$ μm. In order to study the deep drawing with a high coefficient of friction at the punch side, three punches were made with relative clearance 0.9, 0.8 and knurled allover to give a rough surface finish (the knurl roll was of pitch 0.5 mm). The three rough punch stems have become with nominal square side lengths 39.3, 40.0, and 40.5 mm.

As seen in Figure 2, the die is of two zones. The upper is a conical zone with a 36° cone angle that ends with the lower square-aperture zone with side length 44 mm and 10 mm die corner radius. The die has been made of alloy steel and hardened in the same way of hardening the punches, reaching for a value of 60 Rockwell C. After grinding and polishing the surface roughness has been attained to 1.9 μm.
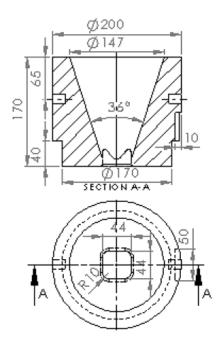
Figure 2: Used die (Dimensions in mms)

2.3. Material properties

The used sheet metals have been from three different materials in different nominal thicknesses. Half hard aluminum (Al99.5w) and brass alloy (67/33 Cu-Zn) sheets have been used in nominal thicknesses 1.0, 1.5, 2.0, 2.5 and 3.0 mm. Annealed aluminum sheets have been used in nominal thickness 2.0, 2.5 and 3.0 mm. Sheet tensile specimens of gage length 50 mm and width 20 mm have been subjected to standard tensile tests under continuous loading up to failure; at least three specimens for each direction. The yield strength has been determined applying the 0.2% offset method. The stress-strain relation has been determined from the curve fitting of the obtained stress-strain values by applying at least 18 stress-strain values in the range of uniform elongation (10 % < ε < maximum uniform strain). The normal ($\bar{r}$) and planar (Δr) average anisotropic coefficients of the used sheet metals are calculated by applying volume constancy law and measurement of length and width strains at 20% longitudinal strain. Table 1 summarizes the average values of the measured mechanical properties of the materials of the used sheet metals.

2.4. Lubrication and friction

The desired conditions of friction at the blank-die interface surfaces are different from that at the blank-punch interface surfaces. While low friction at the surfaces of the blank-die interface facilitates the flow of the blank metal, dry friction between the punch and blank is necessary to increase the frictional force. Therefore, commercial grease has been used as a lubricant at the surfaces of the blank-die interface. The friction coefficient (μ) has been determined by using the plane strain compression test. This test has been carried out using two pairs of hardened high-carbon steel indenters and flat specimens of sheet metals having widths 5.69 and 40.0 mm, respectively. Coefficients of friction (μ) are then calculated using the following equation [23,24].

$$\frac{P_{av}}{\bar{\sigma}} = \frac{\sqrt{3}.e^{\left(\frac{\mu b}{t}\right)-1}}{2\mu(b/t)} \qquad (1)$$

The average pressure, P_{av}, and effective strain, $\bar{\varepsilon}$, for each incremental deformation are

calculated using the following relations.

$$P_{av} = \frac{F}{wb} \qquad (2)$$

$$\bar{\varepsilon} = \frac{2}{\sqrt{3}} \varepsilon_t \qquad (3)$$

Where; $\varepsilon_t = ln\frac{t}{t_o}$

$\varepsilon_t \equiv$ Thickness strain

$F \equiv$ Indenter load

$w \equiv$ Average current specimen width

$b \equiv$ Indenter width

$t \equiv$ Current thickness of specimen

$t_o \equiv$ Initial thickness of specimen

Table 1: Mechanical properties of the materials used.

Material	Stress–strain relation σ (MPa)	Average normal anisotropy $\bar{r}$	Average planar anisotropy Δr	Young's modulus E (GPa)	Poisson's ratio
Brass (CuZn37)	$\sigma = 596\varepsilon^{0.39}$	0.8	0.06	97	0.34
Half hard aluminum (AL99.5w)	$\sigma = 167\varepsilon^{0.066}$	0.6	0.32	66	0.3
Annealed aluminum (AL99.5w)	$\sigma = 126.9\varepsilon^{0.229}$	0.6	0.429	66	0.3

The effective stress $\bar{\sigma}$ corresponding to the calculated value of the effective strain is obtained from tensile stress strain data. Table 2 summarizes the averages of the measured values of the coefficients of friction for the used materials.

Table 2: Average coefficients of friction for the used materials

Material	μ_d (at blank/die interfaces)	μ_p (at blank/punch interfaces)
Half hard aluminum	0.044	0.215
Annealed aluminum	0.018	0.184
Brass	0.033	0.174

3. Finite Element Modeling

Deformation analysis for the process of deep drawing with simultaneous corrective ironing is associated with the difficulty in predicting the following parameters:

1. The loads acting on the drawing tools (both punch and die) and the deformed blank, especially the friction forces acting on the tools-blank interfaces.
2. The limiting drawing ratios LDR.

The load of the punch head and frictional resistance on the punch surface in both the ironing zone and after ironing represent three components of the total punch load [25]. FE analysis would provide a prediction of the total forces acting on the drawing tools and LDR in this combined process.

Drawing a square cup can be simply described as using a flat ended square punch to smoothly push a circular blank through a conical die ending with a square-aperture die cavity. This is pictorially represented in Figure 3.
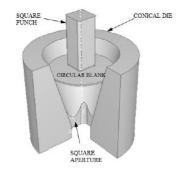

Figure 3: Square-cup drawing process; pictorial representation.

In Figure 4 the initial FE mesh of the blank and drawing sets is presented. The drawing tools: square punch and die, have been modeled as rigid shell with surface-to-surface contact for the interface between the circular blank and the tooling, while the circular blank has been modeled using 4-node shell elements. The strain hardening of the blank

material has been modeled by the power law $\sigma = K\varepsilon^n$ with different values of both the strain hardening coefficient K and strain hardening exponent n. The blank has been simulated by shell elements in all calculations except for the cases of simultaneous corrective ironing, where solid elements have been used. The deformation process has been simulated by imposing a rigid motion to the punch while the die is fully constrained. To represent the non-linear behavior of sheet material a piecewise linear stress-strain curve has been employed, following the tension test data.

Figure 4: FEM mesh of square punch, conical die, and circular blank.

٤.Results and discussion

4.1 Optimum process parameters

Finite element simulation for the developed drawing process has been carried out. The optimum setup dimensions and process parameters have been investigated for half hard aluminum and brass blanks. Table 3 summarizes the optimum process parameters obtained by FE simulations**.**

Table 3: Optimum process parameters obtained by FE simulations.

Process Parameter	Studied values	Optimum value(s)
die angle, α	10, 15, 18, 25, 35, 45, and 90°	18°
die throat length	3, 7, 10 and 13 mm	3-7 mm
die corner radius, r_2	5, 7, 10, 15 and 22 mm	7-10 mm
die fillet radius, r_f	0, 3, 5, 10 and 15 mm	5 mm
punch profile radius, r_p	1, 5, 9, 13, 17 and 19 mm	5 mm
punch corner radius, r_1	2, 4, 7, 12 and 19 mm	4-7 mm
shape factor, r_1/l_1	0.05, 0.1, 0.18, 0.3 and 0.5	0.1-0.2
blank thickness, t_o	1.0, 1.5, 2.0, 2.5 and 3 mm	2-3 mm
coefficient of friction at die-blank interface, μ_d	0.05, 0.1, 0.2 and 0.3	≤0.1
coefficient of friction at punch-blank interface, μ_p	0.1, 0.15, 0.2, 0.25 and 0.3	≥0.2
relative die clearance, c/t_o	1.5, 1.2, 1.0, 0.9, 0.8 and 0.7	≤0.9 for $\mu_p \geq 0.2$

4.2 Deep drawing loads

Variation of the deep drawing punch load with the punch displacement has been investigated and the load-punch-displacement curves are displayed in Figures 5 through 7. Against each value of the punch displacement, in mm, there would be two values for the punch load; one is experimentally measured, in kN, and one is predicted from the finite element simulation (FES-predicted). This has been applied using half hard aluminum, annealed aluminum, and brass blanks; Figures 5, 6 and 7, respectively.
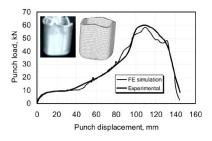

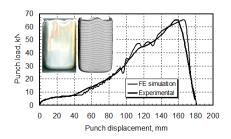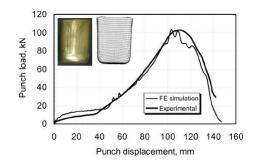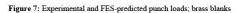**Figure 5:** Experimental and FES-predicted punch loads; half hard aluminum blanks

Figure 6: Experimental and FES-predicted punch loads; annealed aluminum blanks

Figure 7: Experimental and FES-predicted punch loads; brass blanks

The three figures show the gradual increase of the punch displacement that is associated with the deformation of the blank and gradual increase in the punch load. This association continues to the peaks of the curves, where the maximum values of the punch load are reached. These peak values are corresponding to the punch displacement where the partially deformed, by bending, blanks start entering the squared shape die throat. After their peak values, the punch loads decrease as the punch displacements increase.

The figures show how the FES-predicted values of the punch loads are close to the corresponding experimentally measured values.

4.3 Combined effect of relative die clearances and blank thickness on limiting drawing ratio.

Variation of the limiting drawing ratio (LDR) with the relative die clearance has been investigated at three different blank thicknesses. Results have been illustrated in Figures 8 and 9; for half hard aluminum and brass blanks, respectively.
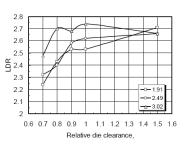

Figure 8: Combined effect of relative die clearances and blank thickness on the limiting drawing ratio of half hard aluminum blanks.
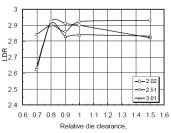

Figure 9: Combined effect of relative die clearances and blank thickness on the limiting drawing ratio of brass blanks.

The two figures indicate that the direct proportion between LDR and the relative die clearance exists in some intervals of the clearance for some blank thicknesses, missed, and inversed in other intervals and/ or thicknesses. However, it can be concluded that the optimal relative die clearance, in which the highest LDR's are obtained, lies in the range $0.9 \leq c/t_o \leq 1.5$ for the half hard aluminum and in the range $0.8 \leq c/t_o \leq 1.0$ for brass blanks.

For instance, in the range $0.8 \leq c/t_o < 1.0$ for brass the cup thickness distribution also is better than the distribution at $c/t_o = 1.5$.

4.4 Limiting drawing ratio

Values of LDR that are theoretically obtained applying the FE simulation model (FES-predicted) have been compared with their corresponding actual values that are experimentally obtained. The comparison has been done for the three used material, of which the

mechanical properties and coefficients of friction are presented in Tables 1 and 2, respectively. Results are summarized in Table 4.

Table 4: Experimental versus FES-predicted LDR's for deep drawing of half hard aluminum, brass, and annealed aluminum

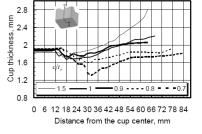| Operating conditions					LDR	
Ironing	c/t_o	Material	t_o	μ_p	FES-Predicted	Experimental
Without ironing	1.5	Half hard aluminum	1.91	0.044	3.00	2.71
	1.5	Brass	2.51	0.033	3.05	2.94
With ironing	0.8	Half hard aluminum	3.02	0.088	2.65	2.70
	0.9	Brass	2.02	0.066	2.85	2.90
				0.174	3.02	2.99
	0.8	Annealed aluminum	3.02	0.036	2.72	2.76
				0.184	3.10	2.93

The last two columns to the right of Table 4 show how the differences between the FES-predicted and experimental values of LDR are not significant, for all the operating conditions. Statistically, a t-test has been done, at a 0.01 level of significance, on the seven paired observations of LDR in Table 4 ending with the conclusion that the differences are not significant. However, some of the minor differences between the FES-predicted and experimental values of LDR's come from using isotropic Von Mises yield criteria which does not take the effect of material anisotropy. In addition, the FES-predicted values have been obtained considering the values of both μ_p and μ_d to be constants. Also, some errors in the setup and used blank may be a source of those minor differences.

Experimental value of LDR for annealed aluminum, in Table 4, has moved up from 2.90 to 2.99 as the value of μ_p has been increased from 0.036 to 0.184. LDR for brass has moved up from 2.76 to 2.93 as the value of μ_p has been increased from 0.066 to 0.174. This leads to conclude that using rough punches

enables obtaining LDR's higher than those obtained by smooth punches. Improving the lubrication condition at the die side as well enhances the increase of the obtained LDR.

4.5 Cup thickness distribution

Figures 10 and 11 show the change of cup thickness measured from the cup center towards the side wall at 90° and 45° with respect rolling direction under different relative die clearances for brass.

Figure 10: Effect of relative die clearances on cup thickness distribution at direction 90° of brass cups ($t_o = 2.02$ mm, BD=107 mm).
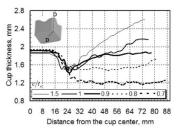

Figure 11: Effect of relative die clearances on cup thickness distribution at direction 45° of brass cups ($t_o = 2.02$ mm, BD=107 mm).

The used blanks were of 107 mm diameter and 2.02 mm initial thickness. The wall thickness has been measured under different relative die clearances; 1.5, 1.0, 0.9, 0.8 and 0.7, at 90° and 45° with respect rolling direction (the marked directions at the middle side wall and the cup corner, respectively). The changes of thickness have been measured at intervals of 2 mm by using a micrometer of $10\ \mu m$ accuracy.

In the two figures, it is clear that: thickness is directly proportional

with the relative die clearance, thickness of the cup bottom is approximately uniformly distributed, and the minimum thicknesses have almost been around the radius of the punch profile.

The use of simultaneous corrective ironing leads to a reduction in the observed change in thickness along the cup wall length. As known, the decrease of the wall thickness by ironing leads to an increase of the useful cup height.

Figure 12 shows the distributions of cup wall thickness in three directions; at 90°, 22.5^o, and 45° with respect to the rolling direction of the brass blank. The three directions are marked as T, M, and D, respectively. The lowest value of the cup thickness was found at the 45° with respect to the rolling direction. This decrease in thickness can be attributed to the tension and circumferential compressive stresses at the punch corner.
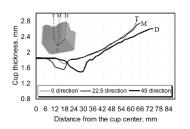
Figure 13 displays the cup thickness distribution over the cup length, measured from the cup center in the 90° direction, as obtained from the experimental results and from the FES (FES-predicted). The comparison has been carried out for a relative die clearance, $c/t_o = 1.5$ and a blank thickness, $t_o = 2.02$ mm for brass. Figure 14 displays the same comparison of the results in the 45° direction. As shown in these two figures there are small differences between FES-predicted and experimental results. Even though, similar trends and good agreements are obtained. The differences can be explained by FES approximation of geometrical setup and working conditions, such as surface roughness and coefficient of friction. However, it is possible to enhance the agreement in results of the two methods by taking a higher order element and including the effect of material anisotropy in the simulation model.

Figure 12. Effect of relative die clearances on cup thickness distribution at directions 90°, 22.5° and 45° of brass cup ($t_o = 2.02$ mm, BD=107 mm, $c/t_o = 1.5$).
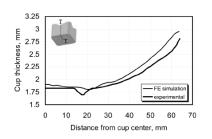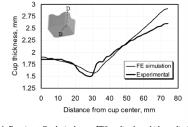

Figure 14. Experimentally-obtained versus FES-predicted cup thickness distribution at direction 45° for brass ($c/t_o = 1.5$, $t_o = 2.02$ mm and DR=2.82).

4.6 Cup height

Figures 15-16 show the variations of cup height versus relative die clearances of half hard aluminum and brass respectively. Cup height has been measured under different relative die clearances at eight points (peak and valley) for each. The cup height has been found

Figure 13. Experimentally-obtained versus FES-predicted cup thickness distribution at direction 90° for brass ($c/t_o = 1.5$, $t_o = 2.02$ mm and DR=2.82).

increasing as the relative die clearances decreasing. The decrease of the thickness by ironing leads to a useful cup height. The usable cup height slightly increases with the decrease of the relative die clearances or increasing the ironing ratio.
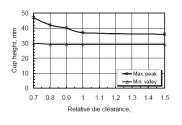

Figure 15. Variation of cup height versus relative die clearances of half hard aluminum cups ($t_o = 1.91$ mm, BD=90 mm).
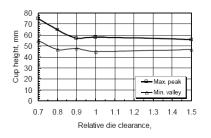

Figure 16. Variation of cup height versus relative die clearances of brass cups ($t_o = 2.02$ mm, BD=107 mm).

Figure 17-18 show the comparison of experimental and FES-predicted cup heights of half hard aluminum and brass, respectively. The comparison has been carried out on relative die clearance, $c/t_o = 1.5$ and blank thickness, $t_o = 1.91$ mm for half hard aluminum and 2.02 mm for brass. Good agreements are obtained between FES-predicted and experimental results.
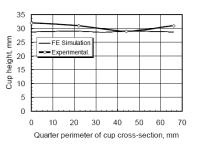

Figure 17. Experimental versus FES-predicted cup heights of half hard aluminum ($c/t_o = 1.5$, $t_o = 1.91$ mm and DR=2.37)
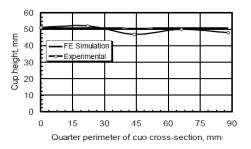

Figure 18. Experimental versus FES-predicted cup heights of brass ($c/t_o = 1.5$, $t_o = 2.02$ mm and DR=2.82)

4.7 Modes of failure

Comparisons of the experimental and FE-predicted modes of fracture for brass and half hard aluminum cups are shown in Figures 19 and 20, respectively. The two figures indicate the effectiveness of the FES technique in predicting the exact location of thinning and wrinkling. This provides the confidence for the developed simulation model as a virtual forming machine. As it has been predicted by the FE simulation, the source of the cup bottom fracture is due to tensile stress, while the source of wrinkling at the cup corners was attributed to the high circumferential compressive stresses.
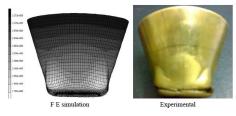
150

Figure 19. FES-predicted versus Experimental modes of failure for drawing brass cup
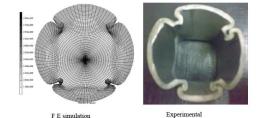(t_o = 2.51 mm, BD=115 mm, DR=2.95 and c/t_o = 1.0).

Figure 20. FES-predicted versus Experimental modes for drawing half hard aluminum cup
(t_o = 1.91 mm, DR=2.60, BD=104 mm and c/t_o = 1.0).

5. Conclusions

The results obtained in this study are summarized below;

1. Applying the developed method using smooth punch, LDR's of 2.92 and 2.74 have been achieved when drawing brass and half hard aluminum square cups, respectively.

2. The LDR has been also increased significantly by using knurled punch with ironing for annealed aluminum and brass blanks. By ironing with knurled punch, the LDR's 3.07 for brass and 2.93 for annealed aluminum were obtained.

3. Effectiveness of ironing with knurled punches is concluded when comparing its resulted LDR=3.07 for brass with the results of the conventional values of LDR=2.3 by using blank holder with all means of improvements while the results of LDR=1.8 without using blank holder [26-28].

4. The range of optimal relative die clearances are $0.9 \leq c/t_o \leq 1.5$ for half hard aluminum and $0.8 \leq c/t_o \leq 1.0$ for brass.

5. The FES-predicted and experimental results showed a good agreement in deep drawing loads, LDR's, thickness distribution, cup height and modes of failure.

REFERENCES

[1] M. Gavas, Increasing the deep drawability of Al-1050 aluminum sheet using multi-point, METALURGIJA, 45 No. 2 (2006) PP. 109–113.

[2] S. A. Sadough, F. Biglari, R. A. Agahi, and M. Shirani, Initial blank design in thermoplastic reinforced sheet drawing based on sensitivity analysis, CIFMA01-IFCAM01, 02–04 max/May, (2006).

[3] Hino, R., Asano, Y., Yoshida, F., and Toropov, V. V., Optimization of blank design for sheet metal forming process using high and low fidelity simulation, 9th AIAA/ISSMO Symposium on Multidisciplinary Analysis and Optimization, 4–6 September, Atlanta, Georgia, (2002).

[4] V. Pegada, Y. Chun, S. Santhanam, An algorithm for determining the optimal blank shape for the deep drawing of aluminum cups, J. Mater. Process. Technol. PP. 125-126 (2002) PP. 743–750.

[5] A. Goel., Blank optimization in sheet metal forming using finite element simulation,

M.Sc. Thesis, Texas A&M University, USA, 2004.

[6] A.C.S. Reddy, Optimization of Blank Shape in Square Cup Deep Drawing Process, https://easychair.org/publications/preprint/TmRN , June 23, 2021.

[7] M.A.M. Basril, H.M. Teng, M. Azuddin, I.A. Choudhury, The effect of heating temperature and methods towards the formability of deep drawn square metal cup ,IOP Conf. Series: Materials Science and Engineering 210 (2017), doi:10.1088/1757-899X/210/1/012067.

[8] P. Yerolkar and C. S. Choudhari, Experimental investigation of forming parameters for deep drawn square part, International Journal of Automobile Engineering Research and Development (IJAuERD) ISSN (P): 2277–4785; ISSN (E): 2278– 9413 Vol. 10, Issue 2, Dec 2020, 9–14.

[9] K. M. Younis, A. S. Jabber, and M. M. Abdulrazaq, Experimental evaluation and finite element simulation to produce square cup by deep drawing process, Al-Khwarizmi Engineering Journal, Vol. 14, No. 1, P.P. 39- 51 (2018).

[10] Jadhav Omkar S., Chirmure Omkar C., Mahekar Sumit S., Gavali Karan R., and Takalkar Atul S., A Review on Different Approaches for Deep Drawing of Square Cup, International Research Journal of Engineering and Technology (IRJET), Volume: 06 Issue: 04 | Apr 2019.

[11] E. Sato, T. Shimizu, T. Sano, and S. Fuchizawa, Effect of multi-axial loading path on limiting drawing ratio, J. Mater. Process. Tech.63 (1997) PP. 60–65.

[12] H. I. Demirci, C. Esner, M. Yasar, Effect of the blank holder force on drawing of aluminum square alloy cup: theoretical and experimental investigation, J. Mater. Process. Technol. 206 (2008) PP. 152–160.

[13] N. Kawai, T. Mori, H. Hayashi, F. Kondoh, Effects of punch cross-section on deep drawability of square shell of Square shell of aluminum sheet, J. Eng. Ind. 109 (1987) PP. 355–361.

[14] Y. Marumo, H. Saiki, T. Mori, Combined effects of strain hardening characteristics and the tool geometry on the deep drawability of square aluminum cups, J. Mater. Process. Technol. 89–90 (1999) PP. 30–36.

[15] L. Lang, Danckert, K. B. Nielsen, X. Zhou, Investigation into the forming of a complex cup locally constrained by around die based on an innovative hydromechanical deep drawing method, J. Mater. Process. Tech. 167 (2005) PP. 191–200.

[16] H. Kim, T. Altan, Q. Yan, Evaluation of stamping lubricants in forming advanced high strength steels (AHSS) using deep drawing and ironing

tests, J. Mater. Process. Technol. 209 (2009) PP. 4122–4133.

[17] L. M. A. Hezam, M. A. Hassan, I. M. Hassab-Allah, M. G. El-Sebaie, Development of a new process for producing deep square cups through conical dies, International Journal of Machine Tools & Manufacture 49 (2009) PP. 773–780.

[18] M. Hassan, L. Hezam, M. El-Sebaie and J. Purbolaksono, Deep drawing characteristics of square cups through conical dies, Procedia Engineering, Vol. 81, 2014, pp. 873 – 880.

[19] L. M. A. Hezam, Deformation characteristics in deep drawing of square cups of sheet metals through conical dies without blank holder, Ph.D. Thesis, Assiut University, Assiut, Egypt,2009.

[20] Abdullah A. Dhaiban, M-Emad S. Soliman, and M.G. El-Sebaie, Development of deep drawing without blank-holder for producing elliptic brass cups through conical dies, Journal of Engineering Sciences, Assiut University, Faculty of Engineering, Vol. 41, No. 4, July 2013,

[21] W. M. Shewakh, M.A Hassan, and I. M. Hassab-Allah, Square-Cup Deep Drawing of Relatively Thick Sheet Metals through a Conical Die without Blankholder, June 2015, International Journal of Materials Forming and Machining Processes 2(2): June 2015, PP. 31-46.

[22] B. Arzamasov, Materials Science, Mir Publishers, Moscow, 1989.

[23] J. M. Alexander, The effect of coulomb friction in the plane compression of a plastic-rigid material, J. Mech. Phys. Solids, Volume 3 (1955) PP. 233–245.

[24] Han, H., Determination of flow stress and coefficient of friction for extruded anisotropic materials under cold forming conditions, Ph. D. Thesis, Royal Institute of Technology, Stockholm, Sweden, (2002).

[25] I. M. Hassab-Allah, A Finite Element Simulation and Experimental Verification of the Deep Drawing of Sheet Metals without Blank-holder with Simultaneous Corrective Ironing, Ph.D., Faculty of Eng., Assiut University, March (1993).

[26] M. Gavas, M. Izciler, Effect of blankholder gap on deep drawing of square cups, J. Mater. Process. Technol. 28 (2007) PP. 1641–1646.

[27] S. S. Han, H. Huh, Modified-membrane finite element simulation of square cup drawing processes considering influence of geometric parameters, J. Mater. Process. Technol. 48 (1995) PP. 81–87.

[28] T. Heinz, and Kaiserplatz, Metal forming practise, Springer-Verlag Berlin Heidelberg, (2006).